

## Supporting Information

### Synthesis and controlled growth of osmium nanoparticles by electron irradiation

Anais Pitto-Barry, Luis M. A. Perdigao, Marc Walker, James Lawrence, Giovanni Costantini\*, Peter J. Sadler\*, and Nicolas P. E. Barry\*

#### Materials and methods

*1. Materials:* The preparations of the complex [Os(*p*-cym)(1,2-dicarba-*closo*-dodecaborane-1,2-dithiolate)] (**1**) and of micelles **OsMs-S** were based on our previous reports.<sup>1,2</sup> The triblock copolymer P123 [poly(ethylene glycol)-*block*-poly(propylene glycol)-*block*-poly(ethylene glycol)] was purchased from Sigma-Aldrich and used as received. Anhydrous tetrahydrofuran (Aldrich) was used. Deionized water (18.2 mega-ohm purity) was collected from a Purelab<sup>®</sup> UHQ USF Elga system. Lacey carbon grids were purchased from Quantifoil Micro Tools GmbH and Elektron Technology UK Ltd, respectively, and used as received.

*2. TEM imaging:* TEM observations were performed on a JEOL 2000FX electron microscope at an acceleration voltage of 200 kV. High magnification TEM images were obtained on a JEOL 2100FX electron microscope at an acceleration voltage of 200 kV. TEM samples were prepared on lacey carbon on 400 mesh gold grids. A drop of sample (5  $\mu$ L) was deposited on the grid and left to air-dry.

*3. XPS measurements:* The x-ray photoelectron spectroscopy (XPS) measurements were conducted on the Kratos Axis Ultra DLD system, with the samples illuminated by a monochromated beam of Al K <sub>$\alpha$</sub>  x-rays ( $h\nu = 1486.6$  eV). Photoelectrons were collected at a take-off angle of 90° (perpendicular to the surface), from an area of approx. 300  $\mu$ m  $\times$  700  $\mu$ m using a hemispherical analyser and a hybrid electrostatic-magnetic lens system. Survey spectra across the full energy range were acquired at a resolution of 1.75 eV. From this, energy regions to be scanned with a resolution of 0.34 eV were determined. Experiments were carried out in ultra-high vacuum conditions and all eight samples were scanned consecutively on the same sample holder. The energy range and transmission function of the system were calibrated using clean Ag foil. Data were analysed using the CasaXPS package, employing mixed Gaussian-Lorentzian (Voigt) lineshapes and asymmetry parameters where appropriate.

The spectra reported in the main paper refer to the spin-orbit-split doublet of the Os 4f peak. In addition to Os, other detected elements were C, B and O, originating from complex **1** and from the block copolymer OsMs micelles. Moreover, three further elements were detected: Si (from the carbon tape), Au (from the mesh of the TEM grid), and F (contaminant from etching of the TEM grid)

*3.1. Reference XPS spectra:* In the study of powders, poor conductors or insulators with XPS it is often necessary to prevent the surface becoming positively charged during exposure to the X-ray beam.<sup>3</sup> As electrons are removed from atoms in the surface region, the surface can become positively charged and this build-up of charge retards the emitted electrons, effectively shifting them to vastly higher binding energies in the acquired spectrum. To compensate for this, the surface is exposed to a beam of low energy electrons (typically a few eV), during the photoemission experiment.

In this study the charge neutraliser of the Kratos Axis Ultra-DLD spectrometer was used, which comprises a filament built in to the entrance of the hemispherical analyser. It was necessary to employ the neutraliser for the powder Os reference samples used to determine the chemical shifts between different Os oxidation states (Fig. 4 in the main paper). The neutraliser parameters were optimised in order to achieve the best experimental resolution prior to the acquisition of data. In the Kratos Axis Ultra-DLD, the optimal resolution is achieved when the sample is slightly over-neutralised (i.e. negatively charged), leading to a downward shift in binding energy of approximately 4 eV which must be compensated for during data analysis. This involves choosing a component which is common to every insulating sample and whose energy is well known. In this investigation, all spectra for the Os reference samples were charge-referenced to the C 1s component at 285.0 eV arising from adventitious carbon on the surface.<sup>4</sup> In order to maintain consistency within the dataset, the spectra acquired from the Os nanoparticle samples were referenced to the same value. This was performed even though these samples did not exhibit surface charging. However, the energy-referencing of the nanoparticle samples led to a binding energy shift of only  $\sim 0.3$  eV from the raw data. Such an approach facilitates the direct comparison of the Os 4f binding energies across all samples and therefore allows an accurate identification of the Os oxidation states of the nanoparticles.

In this comparison we note the binding energy of the Os 4f<sub>7/2</sub> peak reported in the literature for OsO<sub>2</sub> at around 51.7 eV.<sup>5-8</sup> Attention should however be drawn to the fact that these studies use a range of energies for the Au 4f<sub>7/2</sub> peak spanning nearly 1 eV (if they used any charge referencing at all), thereby casting some doubts on the exact energy of the Os 4f<sub>7/2</sub> peak. On the other hand, independently of the absolute values of the Os 4f peaks, our self-consistent approach with reference samples of known oxidation state, allows us to determine precisely the chemical characteristics of the nanoparticles. Indeed, the Os 4f<sub>7/2</sub> binding energies for our reference samples are consistently around 2 eV higher than those reported by White et al.,<sup>5</sup> leading to increased confidence in our assignment of the peak at 53.60 eV as being from OsO<sub>2</sub>, a value consistent with the work of Siedle et al.<sup>8</sup>

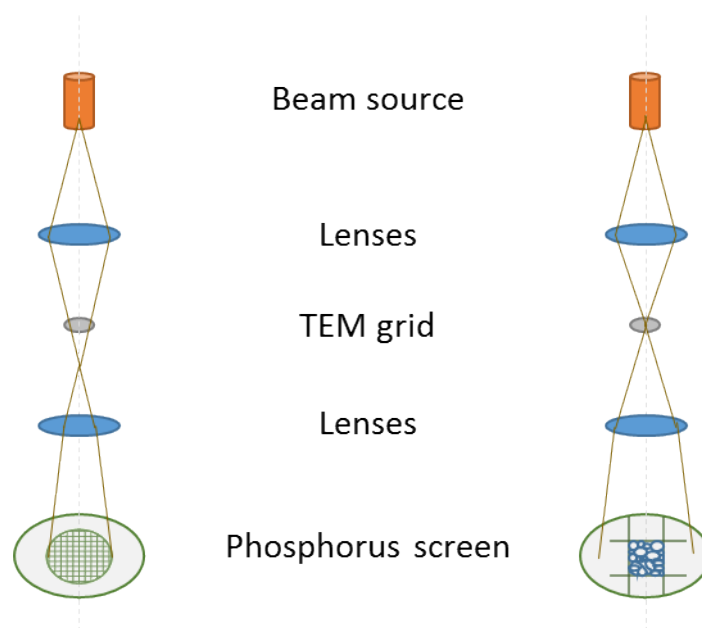


**Fig. S1.** Simplified scheme showing differences between experimental set-up reported here (left; utilisation of a largely spread beam to irradiate the entire grid), and set-up (right, unspread and focused electron beam) as per previously reported.<sup>2</sup>

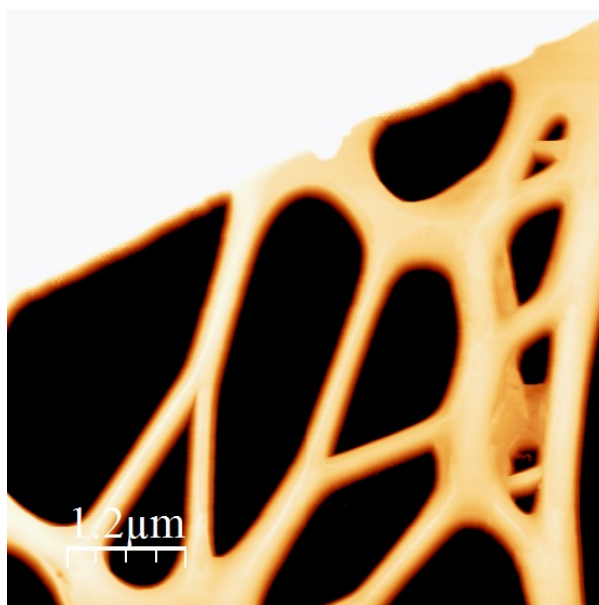


**Fig. S2.** AFM image of a lacey carbon TEM grid prior to any micellar deposition (tapping mode, silicon cantilevers ~60 kHz 3N/m)

1. M. Herberhold, H. Yan and W. Milius, *J. Organomet. Chem.*, 2000, **598**, 142-149.
2. N. P. E. Barry, A. Pitto-Barry, A. M. Sanchez, A. P. Dove, R. J. Procter, J. J. Soldevila-Barreda, N. Kirby, I. Hands-Portman, C. J. Smith, R. K. O'Reilly, R. Beanland and P. J. Sadler, *Nat. Commun.*, 2014, DOI: 10.1038/ncomms4851.
3. J. Cazaux, *J. Electron Spectrosc. Relat. Phenom.*, 1999, **105**, 155-185.
4. J. B. Metson, *Surf. Interface Anal.*, 1999, **27**, 1069-1072.
5. D. L. White, S. B. Andrews, J. W. Faller and R. J. Barnett, *Biochim Biophys Acta.*, 1976, **436**, 577-592.
6. C. K. Rhee, M. Wakisaka, Y. V. Tolmachev, C. M. Johnston, R. Haasch, K. Attenkofer, G. Q. Lu, H. You and A. Wieckowski, *J. Electroanal. Chem.*, 2003, **554-555**, 367-378.
7. Y. Hayakawa, K. Fukuzaki, S. Kohiki, Y. Shibata, T. Matsuo, K. Wagatsuma and M. Oku, *Thin Solid Films*, 1999, **347**, 56-59.
8. A. R. Siedle, R. A. Newmark, G. A. Korba, L. H. Pignolet and P. D. Boyle, *Inorg. Chem.*, 1988, **27**, 1593-1598.